JOURNAL OF MATERIALS SCIENCE 32 (1997) 5233–5242

Fabrication and properties of $YBa_2Cu_3O_{7-\delta}$–Ag composite superconducting wires by plastic extrusion technique

CHAN-JOONG KIM, KI-BAIK KIM, IL-HYUN KUK, GYE-WON HONG
Superconductivity Research Laboratory, Korea Atomic Energy Research Institute, P.O. Box 105, Yusung, Taejon, 305-600, Korea

SOON-DONG PARK, SUK-WOO YANG, HYUNG-SIK SHIN
Department of Chemical Engineering, Chonbuk National University, Chunju, Chonbuk, 560-756, Korea

$YBa_2Cu_3O_{7-\delta}$ (Y123)-Ag composite superconducting wires were fabricated by the plastic extrusion method which involves plastic paste making, die extrusion, binder burn-out and the firing process. The as-extruded Y123-Ag wires were so flexible that they can be easily fabricated into a desirable shape. The current-carrying properties of the wire are dependent on sample size, sintering temperature and silver content. The critical current density, J_c, of the Y123 wire with a large cross-section was lower than that of the wires with a small cross-section, probably due to the large self-induced magnetic field. J_c of the Y123-Ag wires increased with increasing sintering temperature but abruptly decreased above 910 °C, which is close to the eutectic temperature of the Y–Ba–Cu–O system. A silver addition of 10–20 wt% slightly increased J_c of the Y123 (at 77 K and 0 T, it was 140 and 250 A cm^{-2} for the undoped Y123 wire and the Y123 wire with 20 wt% Ag addition, respectively), but further silver addition had a deleterious effect on J_c (180 A cm^{-2} for 30 wt% Ag addition). The small increment in J_c in the Y123 wire with 10–20 wt% Ag addition appears to be due to the enhanced densification and the associated microstructural variation. The decreased J_c of the Y123 wire with 30 wt% Ag addition is considered to be due to the formation of non-superconducting phase, Y_2BaCuO_5 (Y211), $BaCuO_2$ and CuO phases via the decomposition of the Y123 phase.

1. Introduction

Metallic current leads, such as copper or brass, are, in general, used to supply current to the superconducting magnets using liquid helium as a coolant. During current supply, ambient heat is conducted into the cryogenic part through the current leads, owing to the high thermal conductivity of the metallic current leads. When considering the consumption of liquid helium, which is the major portion of the operation cost of the magnets, selection of the current lead material and its shape design are very important. Recently, the replacement by oxide superconductors for the metallic current leads has been attempted [1–7]. As a result of many intensive studies, it was proved that the use of the high-T_c superconductors is effective in reducing the consumption of liquid helium [6, 7], because the thermal conductivity of the oxide superconductor is quite low, and also has no electrical resistance.

Although the critical current density, J_c, of the polycrystalline $YBa_2Cu_3O_{7-y}$ (Y123) superconductor, which was prepared by the conventional sintering method, is as low as a few hundred A cm^{-2}, due to the weak-link properties of the grain boundaries [8, 9], this property level is sufficient to be used as a current lead for the small-scale magnets. Even for the large-scale applications, the large current can be achieved by applying the melt-processing which aligns the superconducting grains to the current travel direction [10, 11].

In order to use this material practically as a current lead, it should be fabricated into a desirable shape. Among the various shape-forming techniques for ceramic materials, the plastic extrusion method is beneficial in mass production. This technique has been applied to the fabrication of the Y–Ba–Cu–O wire with a large cross-section [12, 13]. J_c of the extruded wire was as high as $\sim$1000 A cm^{-2} at 77 K and 0 T, although it decreased with increasing sample size [12]. In addition to the low heat dissipation and the high current-carrying properties, appropriate mechanical properties are required for the current lead application. In order to achieve reliable mechanical properties, incorporation of metal or ceramic into the oxide

0022–2461

superconductor is desirable. Therefore, many attempts have been made to find a promising composite system, and it was found that silver or Ag_2O improves the mechanical properties without serious degradation of the superconducting properties [14–17].

In this work, we prepared Y123–Ag composite superconducting wires by a plastic extrusion technique using organic binders. The processing parameters used to make the Y123–Ag composite wires are reported. The superconducting properties, microstructural characteristics and the reaction between the Y123 phase and the added silver are discussed.

2. Fabrication of Y123–Ag wires

2.1. Powder preparation

The Y123 powder used in this study was prepared by the conventional solid-state reaction method using Y_2O_3, $BaCO_3$ and CuO powder of 99.9% purity. The powders were precisely weighed to a composition of $Y:Ba:Cu = 1:2:3$, ball milled in alcohol for 10 h using ZrO_2 balls (5 mm diameter) and then dried in air. The dried powder mixture was calcined in an alumina crucible at 880 °C in air for 40 h with repeated grinding every 10 h. The calcined Y123 powder was ball milled again for 5 h and then dried in air. Fig. 1a shows a scanning electron micrograph of the prepared Y123 powder. As can be seen, the Y123 powder has an irregular shape and the size is as fine as 2–5 μm. The Y123 powder was mixed with silver powder of 0–30 wt% (High Purity Chemical). The silver powder used is granular in shape and has a size distribution of 2–10 μm (see Fig. 1b).

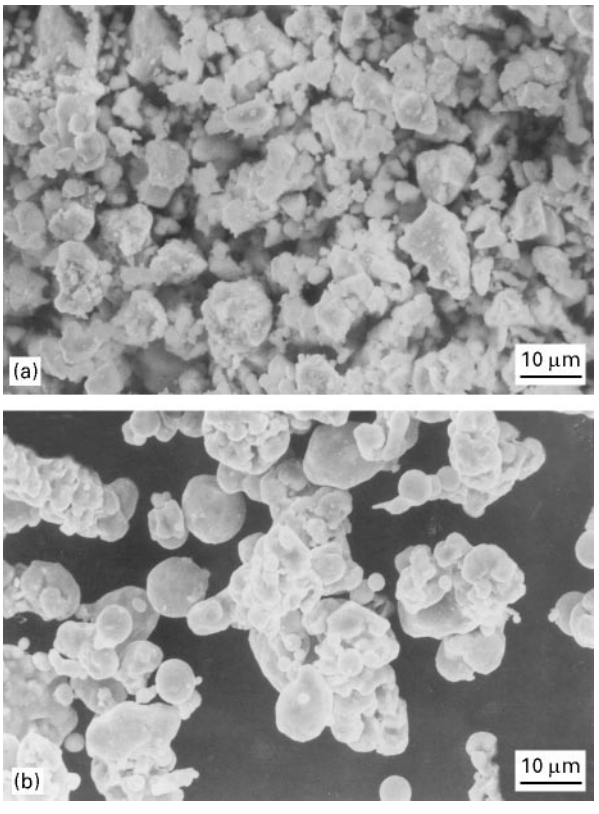

Figure 1 Scanning electron micrograph of (a) the Y123 powder, and (b) silver powder used as a raw material for plastic paste preparation.

2.2. Paste preparation

The fabrication procedure of Y123-Ag composite wires is illustrated in Fig. 2. As the first step, a plastic paste was made by mixing the Y123 powder with various organic binder materials. Ethyl cellulose, glycerol and strearic acid were used as a plastic binder, a plasticizer and a lubricant/dispersant, respectively. The detailed roles of the materials used were described elsewhere [12]. A mixture of ethyl alcohol and butyl carbitol was used as a solvent for the binder materials. The total amount of organic materials was controlled to be less than 5 wt% in order to limit the evolution of porosity during the binder burn-out heat treatment.

The organic binder materials (0.6 g ethyl cellulose, 0.1 g stearic acid and 0.1 g glycerol) were weighed per 20 g Y123–Ag powder and then were dissolved in 100 ml solvent (a mixture of ethyl alcohol and butyl carbitol). The ratio of the two solvent materials was varied and it was found that the viscosity of the mixture was sensitive to the ratio of the two materials. If the viscosity of the paste was low, the paste was not extruded into a continuous body or many microcracks were developed in the as-extruded wire during the drying process after extrusion. At the ratio of ethyl alcohol : butyl carbitol = 9 : 1 or 8 : 2, optimum viscosity was obtained. In order to facilitate the dissolution of the binder materials in the solvent, the solution was heated to 80 °C and then kept for a while. After complete dissolution, the Y123 and silver (silver content 0–30 wt% in 5 wt% steps) powder were taken into the solution and then mixed thoroughly using a magnetic stirrer. Then, the prepared solution was heated to 100 °C in oven and maintained

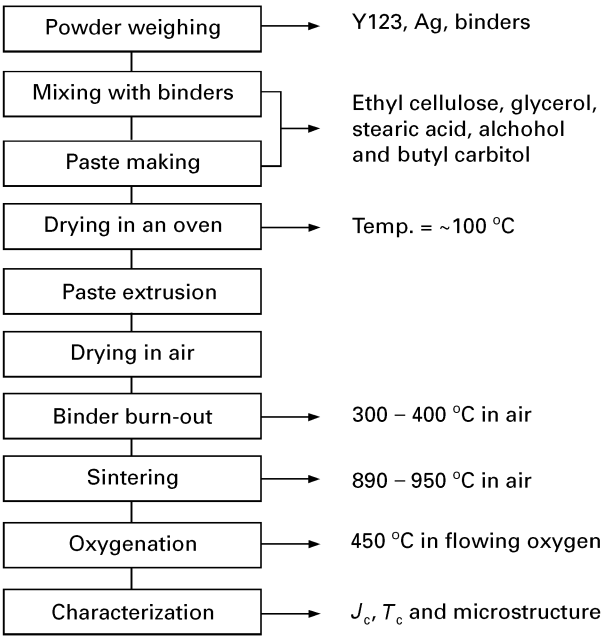

Figure 2 Fabrication procedure for the plastic paste extrusion of Y123–Ag composite wire.

at this temperature for 1 h to remove the solvent material.

2.3. Die extrusion, binder burn-out and firing

The dried paste was loaded into the extrusion die illustrated in Fig. 3 and then extruded into a wire form. Various dies of a 1, 3 and 5 mm diameter were used for extrusion. Fig. 4 shows a photograph of the Y123–Ag wire as-extruded and wound on to a bobbin. The as-extruded wire showed good flexibility, which implies that the ceramic superconductor can be made into various shapes by this method. The extruded Y123–Ag wire was dried for 3–5 h in an ambient atmosphere. In the case of the undoped wire, during drying, microcracks were frequently generated at the sample surfaces while there were fewer microcracks in the samples prepared with silver addition. To determine the condition of the binder burn-out, thermogravimetric (TG) analysis was carried on the dried wire at $P_{O_2} = 0.21$ atm. As can be seen in the TG trace of Fig. 5, a mass change is observed near 300 °C, which is due to the decomposition of ethyl cellulose. In order to remove the binders, therefore, the wire samples were heated to 400 °C in air at a rate of 20 °C h^{-1}, maintained at this temperature for 10 h and then cooled to room temperature at a rate of 50 °C h^{-1}. The Y123–Ag composites were sintered at 890–950 °C for 20 h in air and then annealed at 450 °C in flowing oxygen for 60 h for the tetragonal-to-orthorhombic phase transformation.

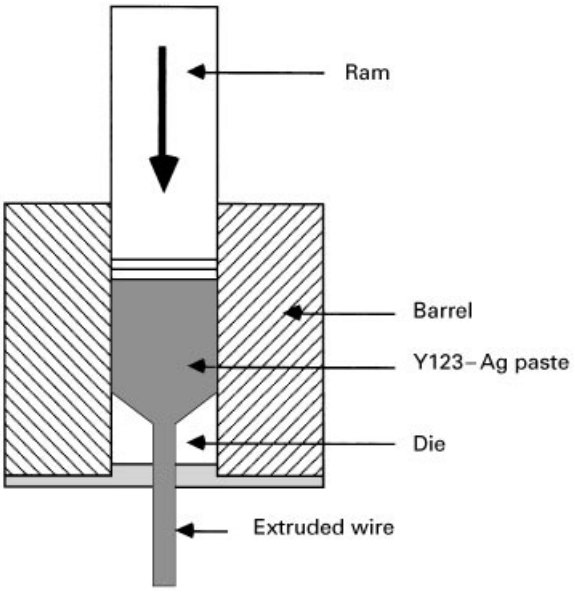

Figure 3 Schematic drawing of plastic paste extrusion.

Figure 4 Photograph of the as-extruded Y123 wire with good flexibility, which was wound on to a bobbin.

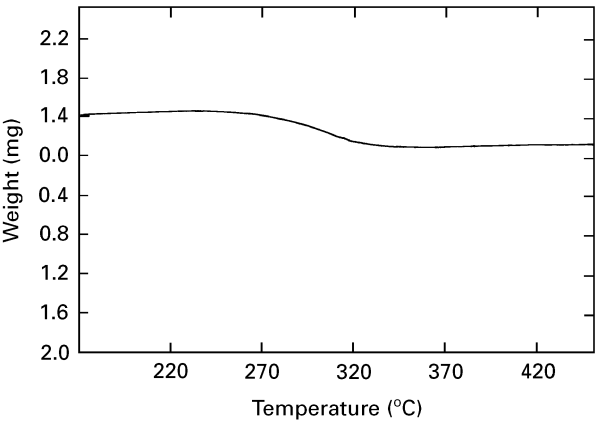

Figure 5 Thermogravimetric trace of the as-extruded Y123 wire. Note the mass change near 300 °C due to the decomposition of ethyl cellulose.

2.4. Characterization of the properties

Phases formed in the calcined and sintered samples were analysed by powder X-ray diffraction method using CuK_α radiation. For microstructural investigation, the sintered Y123–Ag composite wires were mounted using epoxy resin, ground on SiC papers up to 1000 grit and then polished using a diamond paste of 1 μm. The polished samples were etched in 1% HCl (in ethyl alcohol) for 2–5 s and then cleaned in alcohol using an ultrasonic vibrator. Microstructure of the polished and the etched surfaces was investigated by means of an optical microscope and SEM. Superconducting transition temperature, T_c, J_c and critical current, I_c, at 77 K were estimated using a four-probe transport method with indium solder.

3. Results and discussion

3.1. Current properties of the undoped Y123 wires

I_c and J_c of the undoped Y123 wires were measured at 77 K and 0 T. The samples were extruded in 2, 3 and 5 mm dies and sintered at 900 °C in air for 20 h, with subsequent oxygenation annealing at 450 °C for 60 h in flowing oxygen. After sintering, the sample diameters were reduced to 1.5, 2.3 and 4.4 mm, respectively. I_c and J_c results of the two samples are shown in Fig. 6. The I_c values of the Y123 wire with diameters of 1.5, 2.3 and 4.4 mm were 3.85, 8 and 32 A, respectively. J_c of the samples were 220, 160 and 53 A cm^{-2}, which

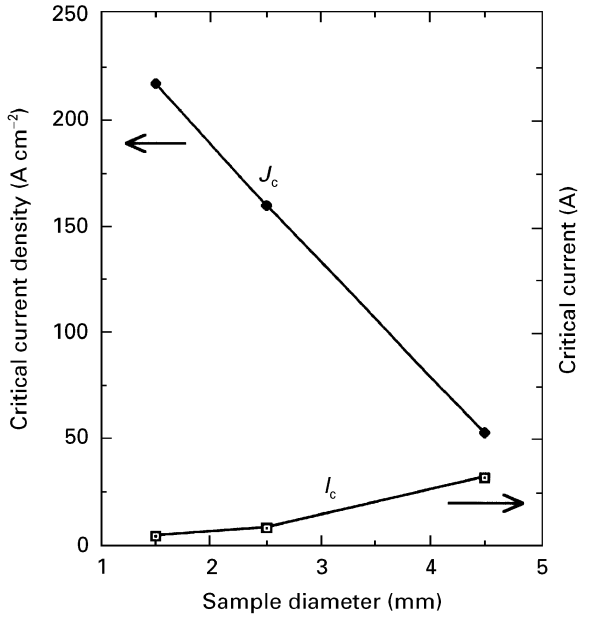

Figure 6 Critical current density, J_c, and critical current, I_c, of Y123 wires as a function of sample size, at 77 K and 0 T.

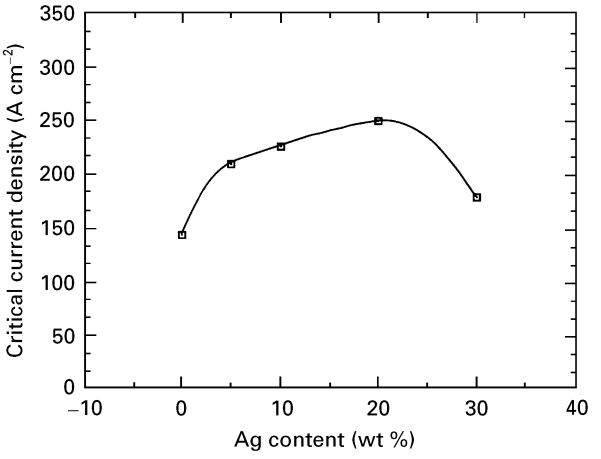

Figure 7 Critical current density, J_c, at 77 K and 0 T of a 2.5 mm diameter Y123–Ag composite wire with silver content.

indicates that the J_c of the sample with a small cross-section is higher than that with a large cross-section. It was reported that the J_c of the sintered Y123 sample was sensitive to the applied magnetic field [8, 18]. According to their results, even at the low magnetic field of 10 Oe, J_c was significantly decreased. This indicates that J_c of the Y123 wires might be influenced by the magnetic field self-induced when current flows into a sample. Such magnetic field limits further current flow and the magnitude depends on the amount of current. Therefore, the low J_c value of the Y123 wire with a large cross-section seems to be due to the larger amount of the self-induced magnetic flux.

3.2. T_c and J_c of Y123–Ag composite wires

T_c and J_c were measured at 77 K and 0 T for the Y123–Ag composite wires with silver contents, which were extruded in a 3 mm die, sintered at 900 °C for 20 h in air and then oxygenated at 450 °C for 60 h in flowing oxygen. T_c of the Y123–Ag composite wires was in the range 91–93 K and no correlation between T_c and silver content was observed. On the other hand, it can be seen in Fig. 7 that J_c slightly increases with increasing silver content and then decreases with further increasing silver content. J_c is about 140, 250 and 180 A cm^{-2} for undoped Y123 wire, the Y123–20 wt% Ag wire and Y123–30 wt% Ag wire, respectively. This indicates that the appropriate amount of silver addition improves J_c of the Y123, but large additions render a deleterous effect on J_c. Similar results were reported in the sintered Y123–Ag/Ag_2O system by Singh *et al.* [17] and by Nishio *et al.* [19]. Referring to Singh *et al.*'s work [17], the J_c increased with increasing Ag/Ag_2O content up to 20 vol% and then decreased at 30 vol% Ag. They explained the J_c decrease at large silver volume fraction by the presence of non-superconducting tetragonal Y123 phase caused by the large silver addition [17]. In this study, however, no tetragonal phase was observed even in the sample with large silver addition. The variation of J_c in this work seems to be related to microstructural variation caused by the silver addition; in particular, the reaction of silver with a Y123 phase to form second non-superconducting phases which will be discussed later.

Fig. 8 shows the variation of J_c at 77 K and 0 T of the Y123–30 wt% Ag wire with sintering temperature. It can be seen that J_c of the sample sintered at 880 °C is about 100 A cm^{-2}, increases to 160 A cm^{-2} on sintering at 900 °C, and then abruptly decreases down to nearly zero when the sintering temperature is higher than 900 °C. The increased J_c with increasing sintering temperature at the low temperature is due to the enhanced densification, while the abrupt decrease of J_c may be related to the eutectic liquid phase that is formed at 923 °C in an air atmosphere [20].

3.3. Microstructure of the undoped Y123 wires

Fig. 9 shows the microstructure of the cross-section of the Y123 wire sintered at (a) 900 °C and (b) 930 °C for 20 h. The samples were extruded in a 3 mm die. As can be seen in the figure, the cross-section of the Y123 sintered at 900 °C is larger than that of the Y123 sintered at 930 °C. Moreover, large spherical pores of 50–200 μm are observed in sample (a). Such pores appears to be formed by gas evolution during binder burn-out heat treatment or by the improper mixing of Y123 powder with the binders. Meanwhile, the microstructure of sample (b) is denser than that of sample (a), as well as having a smaller number of spherical pores.

Fig. 10 shows the optical polarized microstructure of the Y123 wires sintered at (a) 900 °C, (b) 910 °C, (c) 930 °C and (d) 950 °C for 20 h in air and then oxygenated at 450 °C for 60 h in flowing oxygen. It can be seen that the grain size of the Y123 phase depends on the sintering temperature. The Y123 grains of sample (a) are quite small while the large and highly

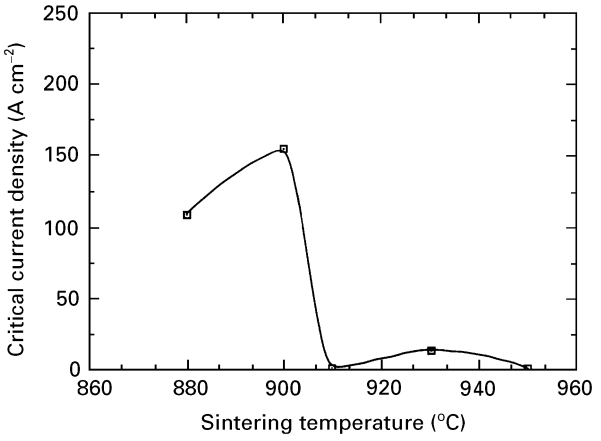

Figure 8 Critical current density, J_c, at 77 K and 0 T of 2.5 mm diameter Y123–30 wt% Ag composite wire with sintering temperature.

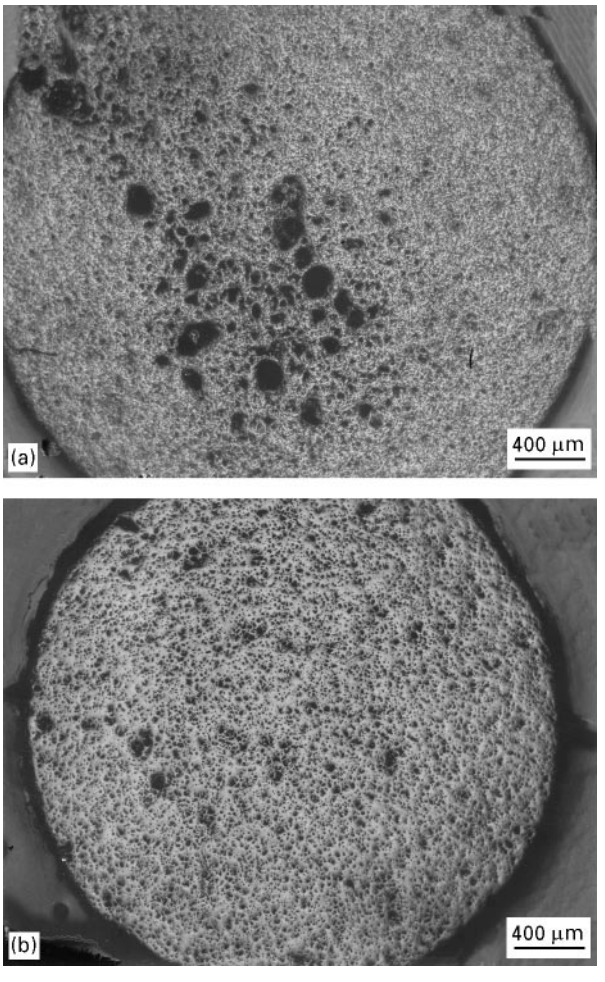

Figure 9 Microstructures of the cross-sections of the Y123 wire sintered at (a) 900 °C and (b) 930 °C for 20 h. Note the evolution of large spherical pores in (a).

anisotropic Y123 grains are developed in the samples sintered at the higher temperatures (Fig. 10c and d). The Y123 grains of the sample sintered at 950 °C are as large as 50–100 μm in length and 20–30 μm thick.

Fig. 11 shows the powder XRD patterns of the Y123 wire sintered at various temperatures of 880, 910 and 950 °C with subsequent oxygenation at 450 °C for 60 h in flowing oxygen. It can be seen that the formed phase in all the samples is an orthorhombic Y123 phase. No other second-phase peaks were observed in the samples prepared in the temperature range 880–950 °C. On the other hand, it should be pointed out that the (0 0 1) texture was developed in the samples sintered at higher temperatures. This is probably due to the fact that the Y123 grains formed in the samples sintered at high temperatures are more anisotropic than those formed at low temperatures, as observed in the microstructures of Fig. 10a–d. By crushing the samples into a powder form to use for the XRD measurement, the Y123 grains might be cleaved on the *a–b* plane, thus creating the texturing effect in the XRD patterns. The texturing effect was more remarkable for the Y123 grains with higher anisotropy. Although no second-phase peaks were observed in the XRD patterns, it cannot be excluded that a very small amount of second phases, which is not detectable within the XRD resolution, was formed in the sample prepared at the high temperature, because the sintering temperature was higher than the eutectic temperature of the Y–Ba–Cu–O system [20].

3.4. Microstructure of Y123–Ag composite wires

Fig. 12 shows the optical microstructure of the Y123 wires extruded with (a) 10 wt% Ag, (b) 20 wt% Ag and (c) 30 wt% Ag addition, which were sintered at 900 °C for 20 h in air and then oxygenated at 450 °C for 60 h in flowing oxygen. It can be seen that the added silver phase (the bright phase) is observed to be dispersed homogeneously within the Y123 matrix. The silver particles appear to be aligned parallel to the extrusion direction. The microstructure of the Y123 wire with a large amount of silver addition is denser than those of the Y123 wires with a small amount of silver additions, because the silver particles filled the pore sites as well as assisted in the densification of the Y123.

Fig. 13 shows scanning electron micrographs of the Y123–30 wt% Ag wire sintered at 880, 930 and 950 °C for 20 h and then annealed at 450 °C for 60 h in flowing oxygen. It can be seen that the microstructure of the sample sintered at higher temperature is denser than that of the sample sintered at low temperature. Many pores are observed in sample (a) but the microstructure of sample (c) is nearly pore-free. In addition, the size of the dispersed silver particles is larger than 10 μm. Compared to the initial size of the silver powder used (2–10 μm), the dispersed silver particles are relatively large, which indicates that grain growth of the silver particles occurred during sintering. In addition to the granular silver dispersion, silver is present as a thin layer at the Y123 grain boundaries (see the regions marked by arrows), but the distribution is not continuous in the boundary region of the Y123.

Fig. 14 shows the powder XRD patterns of Y123–Ag composite (0–30 wt% Ag) wires sintered at 900 °C for 20 h and then annealed at 450 °C for 60 h in flowing oxygen. The main phase formed in all the samples is the orthorhombic Y123 phase. No second-phase formation was observed. In the samples prepared with

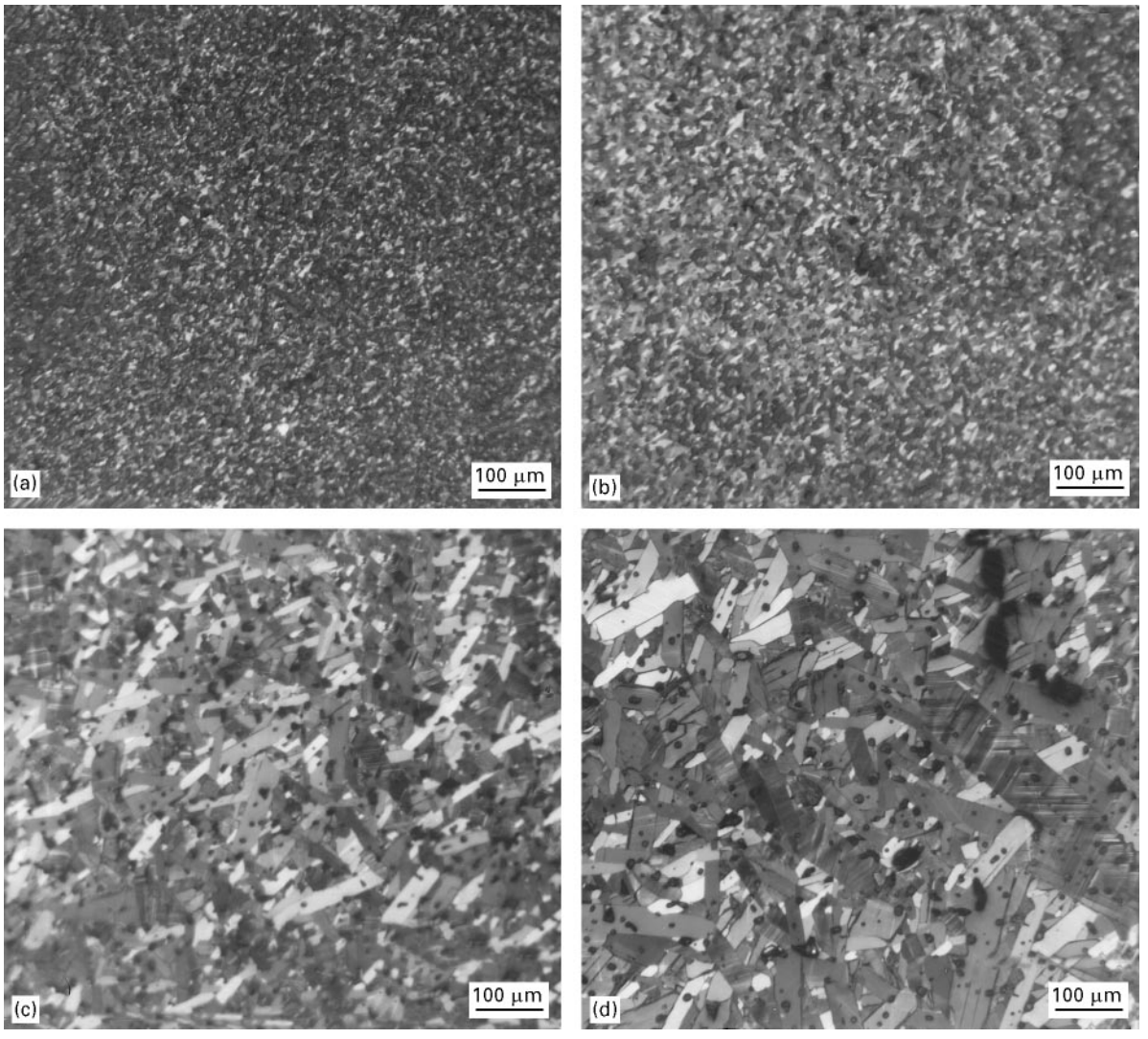

Figure 10 Optical polarized micrographs of the Y123 wire sintered at (a) 900 °C (b) 910 °C (c) 930 °C and (d) 950 °C for 20 h in air, showing the large anisotropic grains in the samples prepared at higher temperatures.

silver addition, silver peaks ($2\theta = 38.06°$, 45.95° and 64.40°) were observed and their intensities increased with increasing silver content.

Fig. 15 shows the powder XRD patterns of the Y123–30 wt% Ag composite wires, sintered at various temperatures (880, 910 and 950 °C), with subsequent oxygenation at 450 °C for 60 h in flowing oxygen. The orthorhombic Y123 peaks and silver peaks are observed. The (0 0 1) texturing is observed in the sample prepared at the higher temperatures. However, the degree of texturing seems to be lower than that observed in the undoped Y123 wire of Fig. 11, which indicates that the silver addition reduced the grain anisotropy of the Y123.

3.5. Reaction between Y123 and silver

Many intensive studies have been performed to understand the effect of silver addition on J_c of a Y123 sample [14–17, 19, 21–28]. As a result, it has been proved that a small silver addition is beneficial to J_c of the sintered Y123, while a large silver addition is deleterous to J_c [17, 19, 24]. In the Y123 samples prepared by creep sintering [25], zone melt-texture growth [26] and hot isostatic pressing [27], silver addition decreased J_c, owing to the formation of non-superconducting phases [27] or Ag–Cu liquid phase [25].

In order to investigate the reaction of a Y123 phase with silver, a simple experimental technique was designed, i.e. coupling of silver compact with a Y123 powder compact (see Fig. 16) and the reaction products at the interface region were examined. The coupled Y123/Ag samples were isostatically pressed in an oil chamber and sintered in the temperature range 890–950 °C for 20 h in air and then cooled in air. The interface region of the coupled samples was easily separated after sintering, owing to the large difference in shrinkage rates and thermal coefficients between the two materials during sintering and the subsequent cooling. Fig. 17 shows a typical example of the separated interface of the coupled Y123/Ag sample which was sintered at 930 °C. It can be clearly seen that green-coloured Y211 phase was observed homogeneously at both interfaces of the sample. Not illustrated here, the Y211 phase was formed at all the interfaces of the samples sintered at 890–950 °C. Fig. 18 shows the XRD results of the interface of the Y123/Ag diffusion

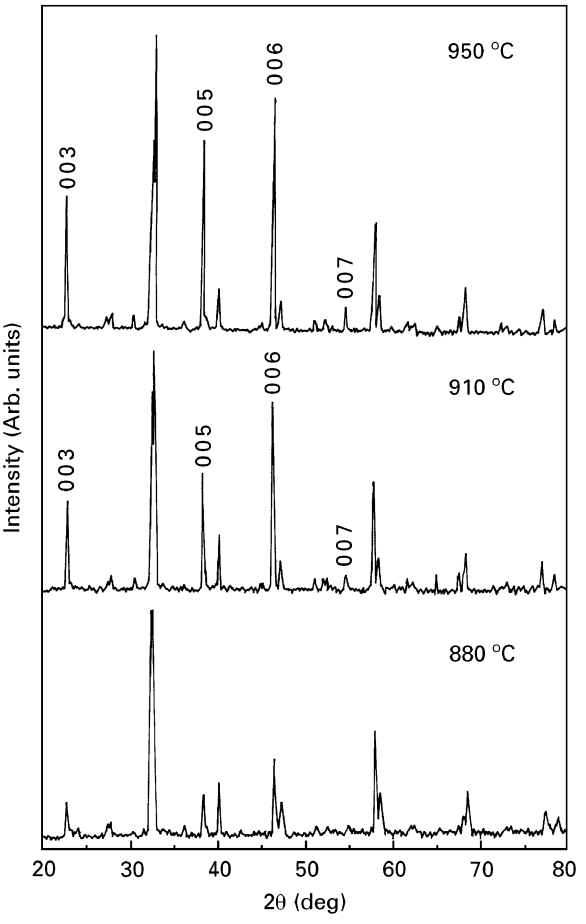

Figure 11 Powder X-ray diffraction patterns of the Y123 wire with sintering temperature. Note the (0 0 1) texturing of the Y123 wire prepared at the high temperatures due to the high anisotropy of the Y123 grains formed.

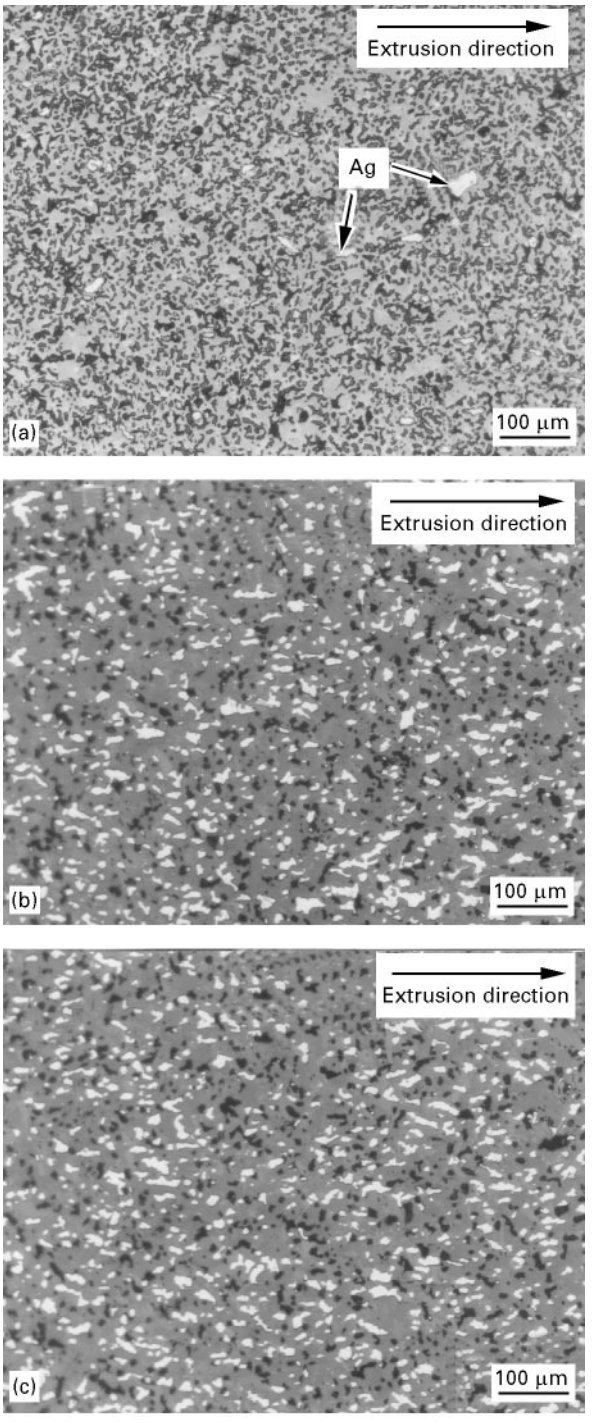

Figure 12 Optical micrographs of the Y123 wire prepared with (a) 10 wt% Ag, (b) 20 wt% Ag and (c) 30 wt% Ag addition. The dark and bright phases are pores and silver particles, respectively. Note that the silver particles are aligned to the extrusion direction.

couple sintered at 930 °C for 20 h; the interface of (a) the silver compact and (b) the Y123 compact. It can be seen in (a) that Y211, CuO and $BaCuO_2$ peaks are observed with the main silver peaks. In (b), the peaks of the Y211 and other second phases are also observed with the main Y123 peaks. This indicates that silver led to the decomposition of a Y123 phase into a Y211 and other second phases under the applied sintering conditions of this study. Although the exact reaction mechanism is not clear, the reaction between silver and a Y123 phase can be inferred as follows

$$2YBa_2Cu_3O_{7-\delta} + Ag \rightarrow Y_2BaCuO_5 + CuO + BaCuO_2 \quad (1)$$

In the Ag–Ba [29] and Ag–Cu [30] binary phase diagram, Ag–Cu liquid phase is developed at 780 °C [30] while the Ag–Ba liquid phase is formed at the lower temperature [29]. Referring to the microprobe analysis studies for the Y123 sintered with silver addition [21], Ag–Cu–O or Ag–Ba–O phases were observed around the solid silver particles in the Y123 matrix, together with other impurity phases. The presence of Ag–Cu–O or Ag–Ba–O phases implies that the composition around the silver particles was off-stoichiometric on the Y123 tie line. The local compositional deviation might lead to the formation of the second non-superconducting phase, such as Y_2BaCuO_5, CuO and $BaCuO_2$. Heat treatment at the higher temperature of 970 °C [23, 28] or applied stress during sintering [25, 27], might accelerate the decomposition reaction of the Y123. Therefore, the decrease of J_c observed in the Y123 samples with a large silver addition is considered to be due to the above reaction. The large silver addition forms a large amount of the second phases which are present as a nearly continuous form at the grain boundaries and the junctions of the Y123. Moreover, when a large

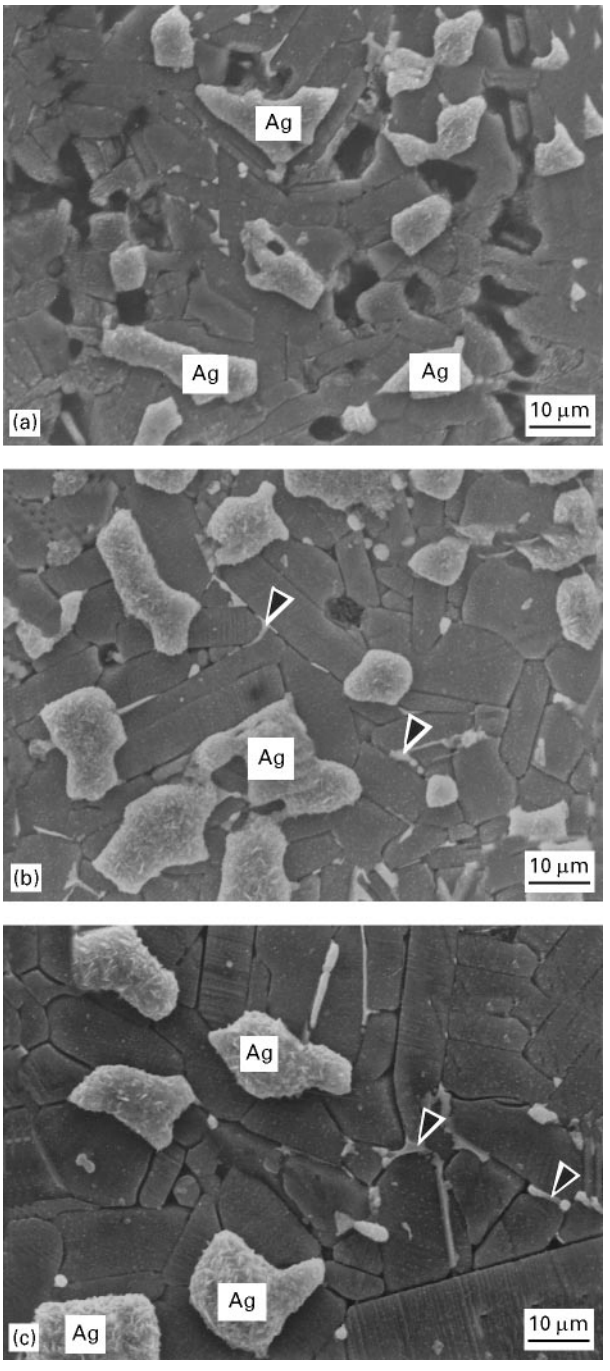

Figure 13 Scanning electron micrographs of the Y123–30 wt% composite wire sintered at (a) 880 °C, (b) 930 °C and (c) 950 °C. Note the presence of silver particles at the grain junctions of the Y123.

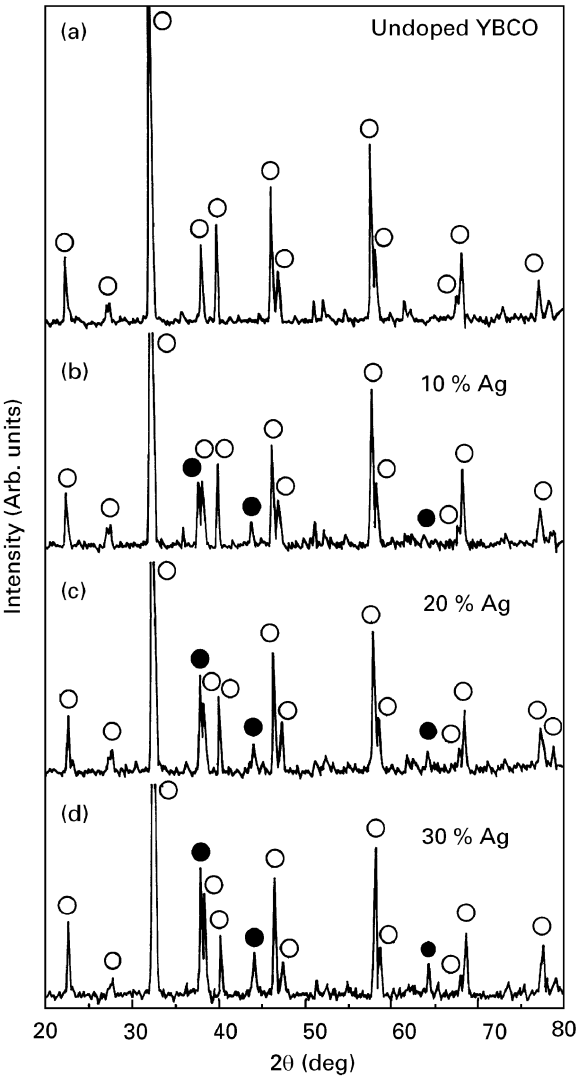

Figure 14 Powder X-ray diffraction patterns of the Y123 wire with (a) no addition, (b) 10 wt% Ag addition, (c) 20 wt% Ag addition and (d) 30 wt% Ag addition. (○) Y123, (●) Ag.

amount of silver is added to the Y123, the volume fraction of the superconducting phase is relatively reduced. These two factors may be responsible for the degradation of J_c of the Y123 wire with 30 wt% Ag addition.

On the other hand, the slight increase of J_c was observed in the sample prepared with silver additions less than 20 wt% and no reaction product was observed in the XRD pattern of the sample. Probably, the kinetics of the reaction between silver and the Y123 is not so fast and the amount of second phase formed might be so small that it could not be detected by the XRD analysis. In this case, the formed phases are considered to be present as a discrete form and hence might not significantly affect the superconducting current travel. Instead, the densification of the Y123 wire was somewhat assisted by the silver addition. The enhanced densification and other microstructural variations, such as suppression of the formation of the microcracks [22] and the possible silver substitution on the copper site [16, 31] would, therefore, lead to the slight increase of J_c in the sample with small silver addition.

4. Conclusions

In this study, Y123–Ag composite superconducting wires were prepared by the plastic extrusion method involving plastic paste making, die extrusion, binder burn-out and sintering. The fabrication parameters of the plastic extrusion were established. The as-extruded Y123–Ag wires were so flexible that they could be easily fabricated into the desirable shape. The J_c of the Y123–Ag wire is dependent on sample size, sintering temperature and silver content. J_c of the sample with a large cross-section was lower than that of wires with a small cross-section, owing to the magnetic flux self-induced when current flows. J_c increased with

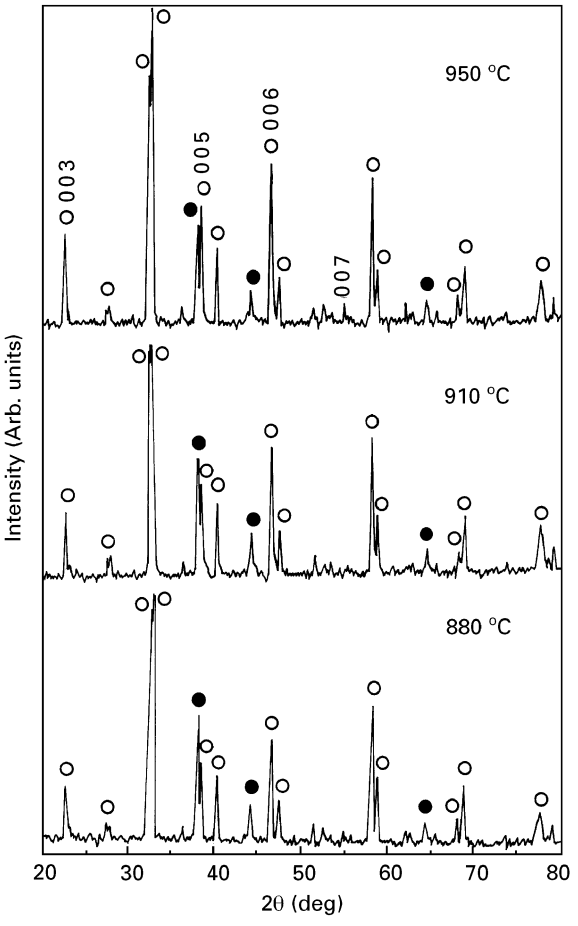

Figure 15 Powder X-ray diffraction patterns of the Y123–30 wt% Ag composite wires, sintered at various temperatures. (○) Y123, (●) Ag.

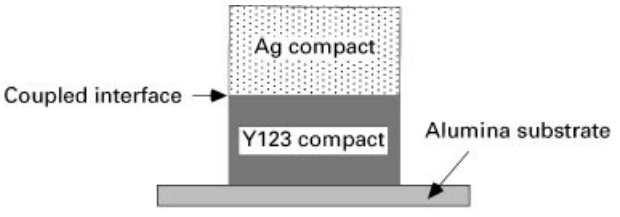

Figure 16 Schematic illustration of the Ag/Y123 coupling experiment.

increasing sintering temperature but abruptly decreased above 910 °C, which is close to the eutectic temperature of Y–Ba–Cu–O system. A silver addition of 10–20 wt% slightly increased J_c of the Y123 (at 77 K and 0 T, it was 140 and 250 A cm^{-2} for the undoped Y123 wire and the Y123 wire with 20 wt% Ag addition, respectively), but further silver addition had a deleterous effect on J_c (180 A cm^{-2} for 30 wt% Ag addition). The small increment of J_c in the sample with 20 wt% Ag addition appears to be due to the enhanced densification and the associated microstructural variation. Meanwhile, the decreased J_c of the sample with large amount of silver addition is considered to be due to the formation of non-superconducting phase, Y211, $BaCuO_2$ and CuO phase via the decomposition of the Y123 phase.

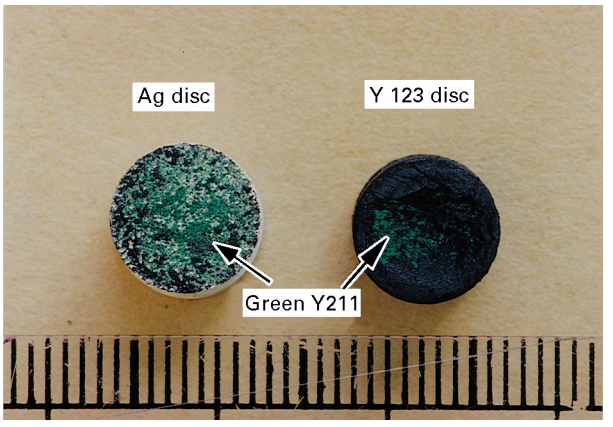

Figure 17 Photograph of the interfaces of the Y123/Ag coupled sample. Note the formation of green Y211 phase at the interface.

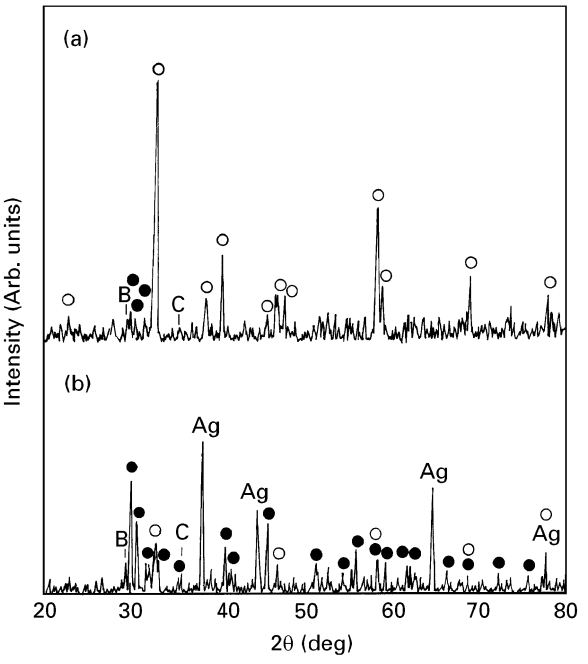

Figure 18 X-ray diffraction pattern for the interface of (a) the Y123 compact, and (b) the silver compact. (○) Y123; (●) Y211; B, $BaCuO_2$; C, CuO.

Acknowledgement

The authors thank the Ministry of Science and Technology (MOST), Korea, for the financial support for this work.

References

1. B. DORRI, K. HERD, E. T. LASKARIS, J. E. TKACZYK and K. W. LAY, *IEEE Trans. Mag.* **27** (1991) 1858.
2. J. L. WU, J. T. DEDERER, P. W. ECKELS, S. K. SINGH, J. R. HULL, R. B. POEPPEL, C. A. YOUNGDAHL, J. P. SINGH, M. T. LANAGAN and U. BALACHANDRAN, *ibid.* **27** (1991) 1861.
3. F. GRIVON, A. LERICHE, C. COTTEVIELLE, J. C. KERMARREC, A. PETITBON and A. FEVRIER, *ibid.* **27** (1991) 1866.
4. R. C. NIEMANN, Y. S. CHA, J. R. HULL, W. BUCKLES and M. L. DAUGHERTY, *ibid.* **30** (1994) 2589.
5. S. Y. SEOL and J. R. HULL, *Cryogenics* **33** (1993) 876.

6. O. KASUU, N. SHIBUTA, K.-I. TAKAHASHI, K.-I. SATO and H. MUKAI, in "Proceedings of the 7th International Symposium on Superconductivity (Advances in Superconductivity VII)", edited by Y. Yamafuji and T. Morishita (Springer, (Kitakyushu, Japan) 1995) p. 839.
7. K. KIMURA, M. SAWAMURA, K. MIYAMOTO, M. HASHIMOTO, K. WATANABE, S. AWAJI and N. KOBAYASHI, *ibid.* p. 851.
8. J. W. EKIN, A. I. BRAGINSKI, A. J. PANSON, M. A. JANOCKO, D. W. CAPONE II, N. J. ZALUZEC, B. FLANDERMEYER, O. F. DE LIMA, M. HONG, J. KWO and S. LIOU, *J. Appl. Phys.* **62** (1987) 4821.
9. J. W. EKIN, T. M. LARSON, A. M. HERMANN, Z. Z. SHENG, K. TOGANO and H. KUMAKURA, *Physica C* **160** (1989) 489.
10. K. SALAMA, V. SELVAMANICKAM, L. GAO and K. SUN, *Appl. Phys. Lett.* **54** (1989) 2352.
11. P. McGINN, W. CHEN, N. ZHU, M. LANAGAN and U. BALACHANDRAN, *ibid.* **57** (1990) 1455.
12. D. PONNUSAMY and K. RAVI-CHANDRA, *J. Mater. Res.* **8** (1993) 268.
13. S. J. GOLDEN, T. YAMASHITA, A. BHARGARVA, J. C. BARRY, I. D. R. MACKINNON and D. PAGE, *Physica C* **217** (1993) 313.
14. L. S. YEOU and K. W. WHITE, *J. Mater. Res.* **7** (1992) 1.
15. F. YEH and K. W. WHITE, *J. Appl. Phys.* **70** (1991) 4989.
16. J. JOO, J. P. SINGH, R. B. POEPPEL, K. GANGOPADHYAY and T. O. MASON, *ibid.* **71** (1992) 2351.
17. J. P. SHINGH, H. L. LEU, R. B. POEPPEL, E. V. VOORHEES, G. T. GOUDEY, K. WINSLEY and D. SHI, *ibid.* **66** (1989) 3153.
18. L. ZUGANG, W. XUEFENG, S. LINJIN, L. MIN, X. HONGWU and Y. NANRU, *J. Mater. Sci. Lett.* **9** (1990) 39.
19. T. NISHIO, Y. ITOH, F. OGASAWARA, M. SUGANUMA, Y. YAMADA and U. MUZUTANI, *J. Mater. Sci.* **24** (1989) 3228.
20. W. WONG-NG and L. P. COOK, *J. Am. Ceram. Soc.* **77** (1994) 1883.
21. S.-H. LIN and N.-L. WU, *J. Mater. Res.* **9** (1994) 1112.
22. B. DWIR, B. KELLETT, L. MIEVILLE and D. PAVUNA, *J. Appl. Phys.* **69** (1991) 4433.
23. M. J. DAY, S. D. SUTTON, F. WELHOFER and J. S. ABELL, *Supercond. Sci. Technol.* **6** (1993) 96.
24. I. DHINGRA, G. K. PADAM, S. SINGH, R. B. TRIPATHI, S. U. M. RAO, D. K. SURI, K. C. NAGPAI and B. K. DAS, *J. Appl. Phys.* **70** (1991) 1575.
25. L. SCHMIRGELD, P. REGNIER, L. CHAFFRON, X. DESCHANELS, F. MAURIS, J. MARUCCO and R. GABILLY, *Supercond. Sci. Technol.* **4** (1991) 327.
26. P. McGINN, N. ZHU, W. CHEN, M. LANAGAN and U. BALACHANDRAN, *Physica C* **167** (1990) 343.
27. G. E. JANG and K. MUKHERJEE, *Supercond. Sci. Technol.* **7** (1994) 344.
28. T. L. WARD, T. T. KODAS, A. CARIM, D. M. KROEGER and H. HSU, *J. Mater. Res.* **7** (1992) 827.
29. G. BRUZZONE, M. FERRETTI and F. MERLO, *J. Less-Common Metals* **128** (1987) 259.
30. T. B. MASSALSKI, J. L. MURRAY, L. H. BENNETT and H. BAKER, in "Binary Alloy Phase Diagram" edited by T. B. Massalsri (American Society for Metals, Metals Park, OH, 1986) p. 19.
31. M. MATSUMOTO, T. ABE, M. TANAKA, T. TAZAWA and E. SATO, *Mater. Res. Bull.* **23** (1988) 1241.

Received 8 December 1995
and accepted 10 March 1997